Supporting Information

Ultrafast Electron Transfer at the $ZnIn_2S_4/MoS_2$ S- Scheme Interface for Photocatalytic Hydrogen Evolution

Himanshu Bhatt[†], Mahammed Suleman Patel[†], Tanmay Goswami[†], Dharmendra K. Yadav[†], Atal Swathi Patra[‡] and Hirendra N. Ghosh[‡, *]

[†]Institute of Nano Science and Technology, Knowledge City, Sector 81, SAS Nagar, Punjab-140306, India

[‡] School of Chemical Sciences, National Institute of Science Education and Research (NISER), Bhubaneswar, Odisha 752050, India

*E-mail: hnghosh@niser.ac.in, hnghosh2004@gmail.com

Experimental Section:

Materials. Zinc chloride ($ZnCl_2$), indium chloride ($InCl_3$), and thioacetamide (TAA) were purchased from Sigma-Aldrich, India. Bulk MoS_2 powder was purchased from Sigma Aldrich.

Preparation of MoS_2 nanosheets. Few-layer MoS_2 nanosheets were synthesized via the liquid exfoliation technique. Initially, 125 mg of bulk MoS_2 powder was finely ground using a mortar and pestle for 30 minutes to achieve a consistent powder form. This powder was then dispersed in 25 mL of ethanol and subjected to ultrasonic treatment for 6 hours in a bath sonicator. The resultant solution, containing exfoliated few-layer MoS_2 nanosheets, was subsequently decanted and reserved for subsequent experimental analysis.

Preparation of $ZnIn_2S_4$ nanosheets. The $ZnIn_2S_4$ (ZIS) nanosheets were synthesized using a hydrothermal method detailed in our previous report.[1] $ZnCl_2$ (1.0 mmol; 0.136 g) is first dissolved in 30 mL of DI water. Following this, $InCl_3$ (2.0 mmol; 0.442 g) was added, with the mixture stirred for 10 minutes. Subsequently, an excess of thioacetamide (TAA) (8.0 mmol; 0.601 g) was introduced, and the solution was stirred for another 15 minutes. Post-stirring, the solution was sonicated for 45 minutes, then placed into a 50 mL Teflon-lined stainless-steel autoclave and heated at 180°C for 20 hours. The resultant yellow product was isolated by centrifugation at 8000 rpm, washed with ethanol several times, and finally dried in a hot air oven at 80°C for about 7 hours.

Preparation of ZIS/MoS_2 heterostructure. The ZIS/MoS_2 heterostructure was synthesized using an in-situ growth technique with modifications from a previously reported method.[2] The preparation of the ZIS/MoS_2 heterojunction was similar to that of $ZnIn_2S_4$ nanosheets, with the key difference being the addition of MoS_2 sheets in specific weight percentages to the ZIS precursors prior to the reaction. For the 2 wt% ZIS/MoS_2 heterostructure, 8.6 mg of MoS_2 was added. Similarly, for creating 5 wt%, 10 wt% and 15 wt% variants, appropriate amounts of

MoS_2 were carefully measured and incorporated, and the resultant composites were termed as ZIS/MoS_2-2, ZIS/MoS_2-5, ZIS/MoS_2-10 and ZIS/MoS_2-15, respectively.

Instrumentation Details.

The powder-XRD measurements were conducted using the BRUKER D8 ADVANCE with Cu-Kα radiation (λ = 1.542 Å). The morphological and microstructure properties of the samples were carried out by employing a Transmission Electron Microscope (TEM, JEOL JEM 2100) operating at an accelerating voltage of 200 kV. A Shimadzu UV-2600 UV-vis spectrophotometer was utilized to acquire the steady-state absorption spectra of the synthesized samples. The elemental analysis of the synthesized materials was investigated using X-ray photoelectron spectrometer (XPS- Thermo Fisher Scientific K-Alpha). A Fluorolog 3-221 fluorimeter was used to record the steady-state photoluminescence spectra.

Photocatalytic hydrogen (H_2) evolution. The hydrogen evolution reactions were conducted in a sealed gas-circulation setup. For each experiment, 10 mg of the photocatalyst was suspended in a 50 mL aqueous solution with 15 vol% triethanolamine (TEOA) serving as a sacrificial agent and stirred continuously. Before solar irradiation, air was removed from the system and then kept in the dark for about 1 hour. Subsequently, the solution was exposed to solar light using a solar simulator (PECCEL, PEC-L01) of power 100mW cm^{-2} (AM-1.5). The produced hydrogen was quantified with the help of gas chromatography (GC-2014) by using thermal conductive detector (TCD).

Ultrafast Transient absorption spectroscopy

A Ti: sapphire amplifier system (Astrella and Coherent) was used to perform transient absorption spectroscopic measurements. This amplifier generates the femtosecond laser pulse with a central wavelength of 800 nm with a pulse energy of 5 mJ and a temporal pulse width of approximately 35 fs, which has a repetition rate of 1 kHz. Along with this, a Helios Fire

pump-probe spectrometer was used to record the transient absorption spectra. The main laser beam was divided into two beams named as the pump and probe beams in the ratio of (70:30) using an efficient beam splitter. The pump wavelength to excite the sample (370 nm) was generated employing an Optical Parametric Amplifier (OPerA-SOLO, model no: TO8U6W). During the experiment, a variable delay to the probe beam was provided using a mechanical delay stage, positioned in its path. The white light continuum probe beam (UV-vis) was generated from 800 nm monochromatic light pulses using CaF_2 crystal. Both probe and pump beams were overlapped at the sample position. The sample was placed in a quartz cuvette with thickness of 2 mm. The CMOS detector was used to detect the transmitted probe and the difference in the absorption of the probe pulse (ΔA) was measured by subtracting the probe absorption in the presence and absence of the pump (A_{pump}-$A_{without\ pump}$). The recorded data was fitted and chirp corrected using the Surface explorer software. The experiments were performed in the solution phase, dispersing all the samples in ethanol, and maintaining similar optical density at 370 nm (excitation wavelength) and 300 μJcm^{-2} pump fluence.

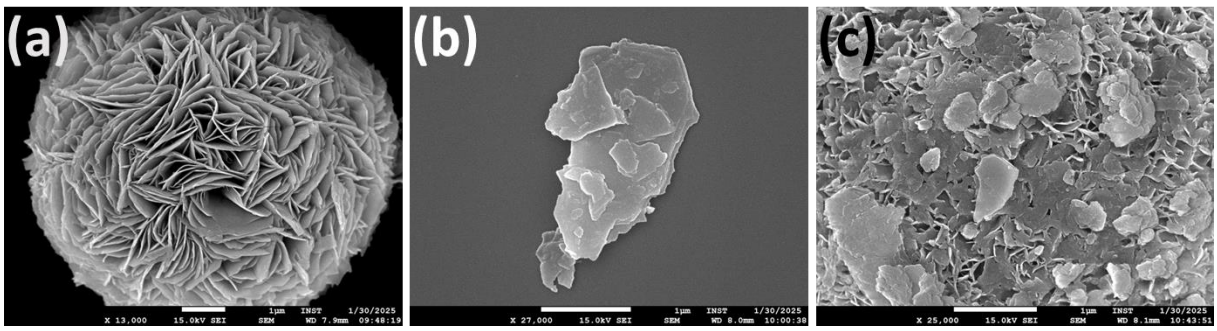

Figure S1. FESEM images of **(a)** ZIS, **(b)** MoS_2 and **(c)** ZIS/MoS_2-10 heterostructure.

Figures S1a, b and c show the FESEM images of the ZIS, MoS_2 and ZIS/MoS_2-10 heterostructure, respectively. The FESEM image of ZIS (Figure S1a) reveals the flower-like

microspheres assembled by the nanosheets. Whereas MoS_2 (Figure S1b) exhibits the nanosheets-like morphology. However, the FESEM image of the ZIS-MoS_2-10 heterostructure (Figure S1c) portrays the presence of both ZIS and MoS_2 nanosheets.

The calculation for solar-to-hydrogen conversion efficiency (STH)

The solar-to-hydrogen conversion efficiency was calculated by using the following expression;[3,4]

$$STH\ (\%) = \frac{r_{H_2} \times \Delta G}{P_{sun} \times A}$$

r_{H_2}, ΔG,P_{sun} and A represents the hydrogen production rate ($mols^{-1}$), Gibbs free energy for water splitting reaction (237 $kJmol^{-1}$), power of incidence solar light (100$mWcm^{-2}$) and irradiated surface area, respectively.

Table S1: Solar-to-hydrogen conversion efficiency and other experimental parameters for ZIS and ZIS/MoS_2-10 heterostructure after the irradiation of solar light for 5h.

System	Irradiation surface area (A) in cm^2	Incidence power (P) in $mWcm^{-2}$	r_{H_2} in $\mu molh^{-1}$	STH in %
ZIS	16.7	100	4.55	0.02
ZIS/MoS_2-10	16.7	100	12.8	0.05

Using the above experimental data, we calculated the STH to be 0.02 % and 0.05% for ZIS and ZIS/MoS_2-10 heterostructure, respectively.

The calculation for apparent quantum efficiency (AQE)

We performed the apparent quantum efficiency (AQE) measurement for both ZIS and ZIS/MoS_2-10 after 400 nm solar irradiation. The experimental data of the measurements are listed below in Table S1;

Table S2: Apparent quantum efficiency and incidence light parameters for ZIS and ZIS/MoS_2-10 heterostructure after irradiating 400 nm light for 5h.

System	Irradiation surface area (A) in cm^2	Incidence power (P) in mW/cm^2	$n_{H_2}(t)$ in µmol	AQY in %
ZIS	16.7	17	1.2	0.02
ZIS/MoS_2-10	16.7	17	16.3	0.20

The apparent quantum efficiency was calculated by using the following expression[5]

$$\text{AQE}\ (\%) = \frac{2 \times n_{H_2}(t) \times N_A \times h \times c \times 100}{P \times A \times t \times \lambda_i}$$

Where, $n_{H_2}(t)$ is the number of moles of hydrogen evolved after the time duration; t, N_A is Avogadro's number (6.022×10^{23}), and P is the power of incidence light. A is the irradiation surface area, h and c represent Planck constant (6.6 x 10^{-34} J-s) and speed of light (3x10^8 m/s). We have used monochromatic light of wavelength λ_i; 400 nm to measure AQE.

With the help of experimental results, the AQE for ZIS and ZIS/MoS_2-10 were calculated to be 0.02 % and 0.20 %, respectively. The higher AQE for heterostructure than pristine ZIS nanosheets suggests the improved charge separation at the S-scheme interface.

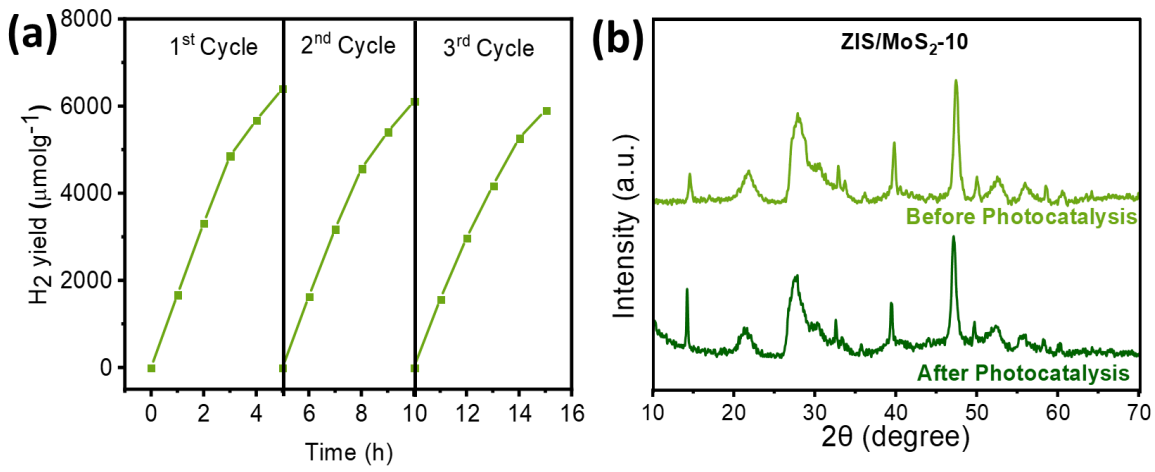

Figure S2. (a) Recycling H_2 evolution activity of ZIS/MoS_2-10 heterostructure for 15h in a 5h cycle. (b) XRD patterns of ZIS/MoS_2-10 before and after photocatalysis.

Table S3. Comparaison of représentative MoS_2, $ZnIn_2S_4$ and S-scheme heterostructure based photocatalysts for H_2 evolution efficiency.

Photocatalysts	**Irradiation source**	**Sacrificial agent**	**H_2 evolution Activity** (mmol g^{-1} h^{-1})	**Reference**
S-scheme $ZnIn_2S4/MoS_2$	Solar simulator 100 mW cm^{-2} (AM-1.5)	TEOA	1.28	**This work**
S-scheme Cu/$ZnIn_2S_4$-V_S/TiO_2-V_O	300 W Xe lamp	N/A	1.25	6
Z-scheme CdS-MoS_2/OCN	300 W Xe lamp	0.25 M Na_2SO_3 and 0.35 M Na_2S	0.638	7
S-scheme $ZnIn_2S_4/WO_3$	300 W Xe lamp (λ>400 nm)	10 vol % methanol	0.30	8
Z scheme TiO_2–$ZnIn_2S_4$	300 W Xe lamp	N/A	0.215	9
S-scheme MoS_2 hollow sphere/$ZnIn_2S_4$ nanosheets	300 W Xe lamp (λ>420 nm)	TEOA	1.07	10
S-scheme COF-$ZnIn_2S_4$	300 W Xe lamp	0.25 M Na_2SO_3 and 0.35 M Na_2S	0.695	11
S-scheme N-doped $CeO_{2-\delta}$@$ZnIn_2S_4$	300 W Xe lamp	0.25 M Na_2SO_3 and 0.35 M Na_2S	0.798	12
Z scheme $ZnIn_2S_{4-x}$-WO_{3-x}	300 W Xe lamp (λ > 420 nm)	N/A	0.738	13
S-scheme N doped MoS_2/S doped g-C_3N_4	300 W Xe lamp	TEOA	0.656	14
Z scheme MoS_2/CoP	300 W Xe Lamp	TEOA	0.077	15

$Ta_3N_5/ZnIn_2S_4$	300 W Xe lamp (λ>400 nm)	0.25 M Na_2SO_3 /0.35 M Na_2S	0.63	16
$CoFe_2O_4/ZnIn_2S_4$	300 W Xe lamp (λ>420 nm)	20 vol% TEOA	0.80	17
Ti_3C_2 MXene@$TiO_2/ZnIn_2S_4$	300 W Xe lamp	N/A (Titanium co-catalyst)	1.18	18
3-CPDs/$ZnIn_2S_4$	300 W Xe arc lamp (λ > 420 nm)	Na_2S/Na_2SO_3	0.133	19
$ZnIn_2S_4$/B-C_3N_4	300 W Xe Lamp (λ > 420 nm)	TEOA (Melamine co-catalyst)	0.876	20
BiOCl@$ZnIn_2S_4$	1000 W Xe Lamp (λ > 420 nm)	N/A (Platinum co-catalyst)	0.674	21
CF@$ZnIn_2S_4$	300 W Xe Lamp	N/A	0.279	22
$Ni_{0.05}$ doped CdS/MoS_2	300W Xe lamp 100 mW cm^{-2}	0.35 M Na_2S and 0.25 M Na_2SO_3	0.825	23
MoS_2/MoO_2	300 W Xe Lamp	Na_2SO_3/Na_2S	0.241	24
MoS_2 sheet/carbon nanofiber	300 W Xe Lamp	TEOA	0.300	25
ZnS/MoS_2	Hg pen-lamp (254 nm, (4.4 mW cm^{-2})	Na_2SO_3/Na_2S	0.606	26
g-C_3N_4-PANI-MoS_2	300 W Xe Lamp (λ > 420 nm)	TEOA	0.594	27

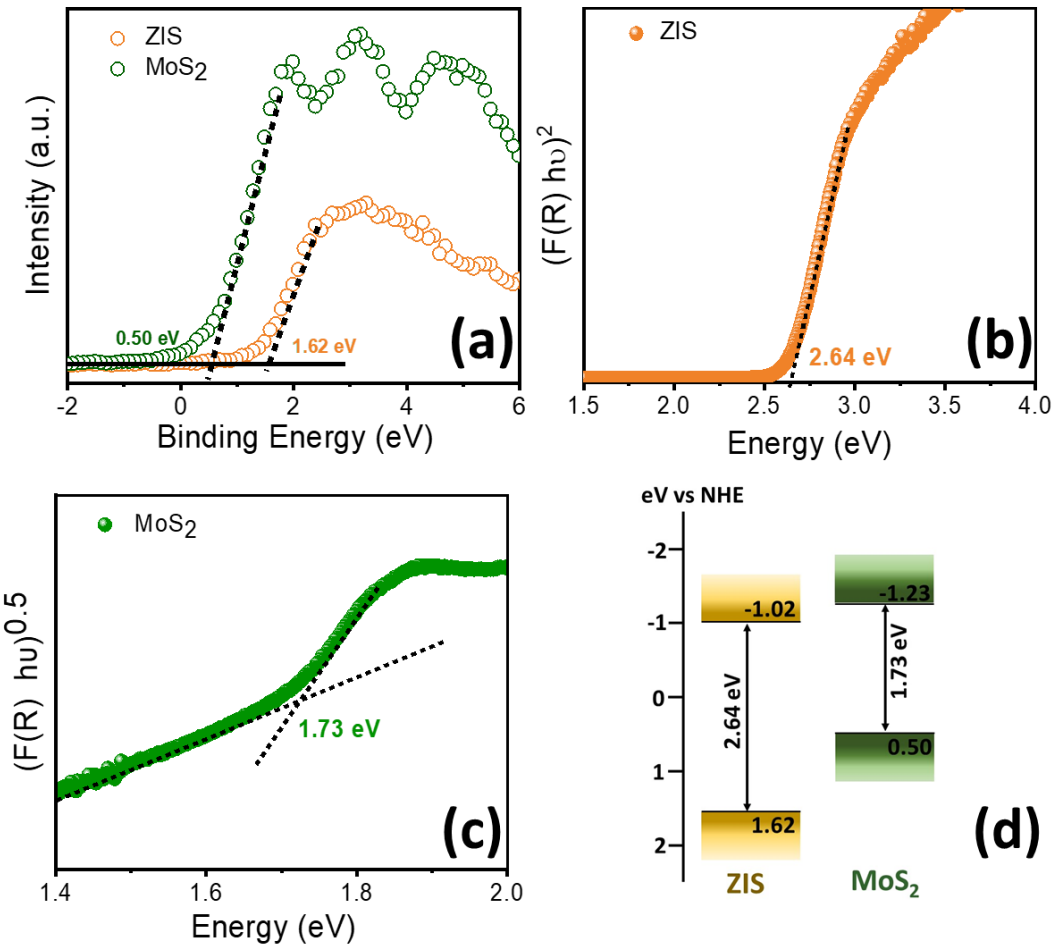

Figure S3: (a) Valence band spectra of ZIS and MoS_2. Tauc plot of (b) ZIS and (c) MoS_2 derived from the respective DRS spectra. (d) band position estimation for ZIS and MoS_2.

Figure S3a shows the VB spectra of ZIS and MoS_2 obtained from the XPS study. The intersection point of the baseline and the leading edge of the spectrum gives the value of the VBM. Therefore, the VBM position of ZIS and MoS_2 was estimated to be 1.62 eV and 0.50 eV vs NHE. Next, the conduction band minima (CBM) was calculated using the following expression,

$$CBM = VBM + E_g$$

where E_g represents the band gap of the material and can be estimated using the Tauc plot derived from the diffuse reflectance spectroscopy (DRS) spectra. Figures S3b and c show the Tauc plot for ZIS and MoS_2, respectively, derived from the respective DRS spectra. The band gap of ZIS and MoS_2 was found to be 2.64 eV and 1.73 eV, respectively. By combining the

respective VBM and E_g values, we obtained the CBM value for ZIS and MoS_2, which is to be -1.02 eV and -1.23 eV vs NHE, respectively. As shown in Figure S3d, the ZIS and MoS_2 are comprised of staggered type band alignment in the heterostructure.

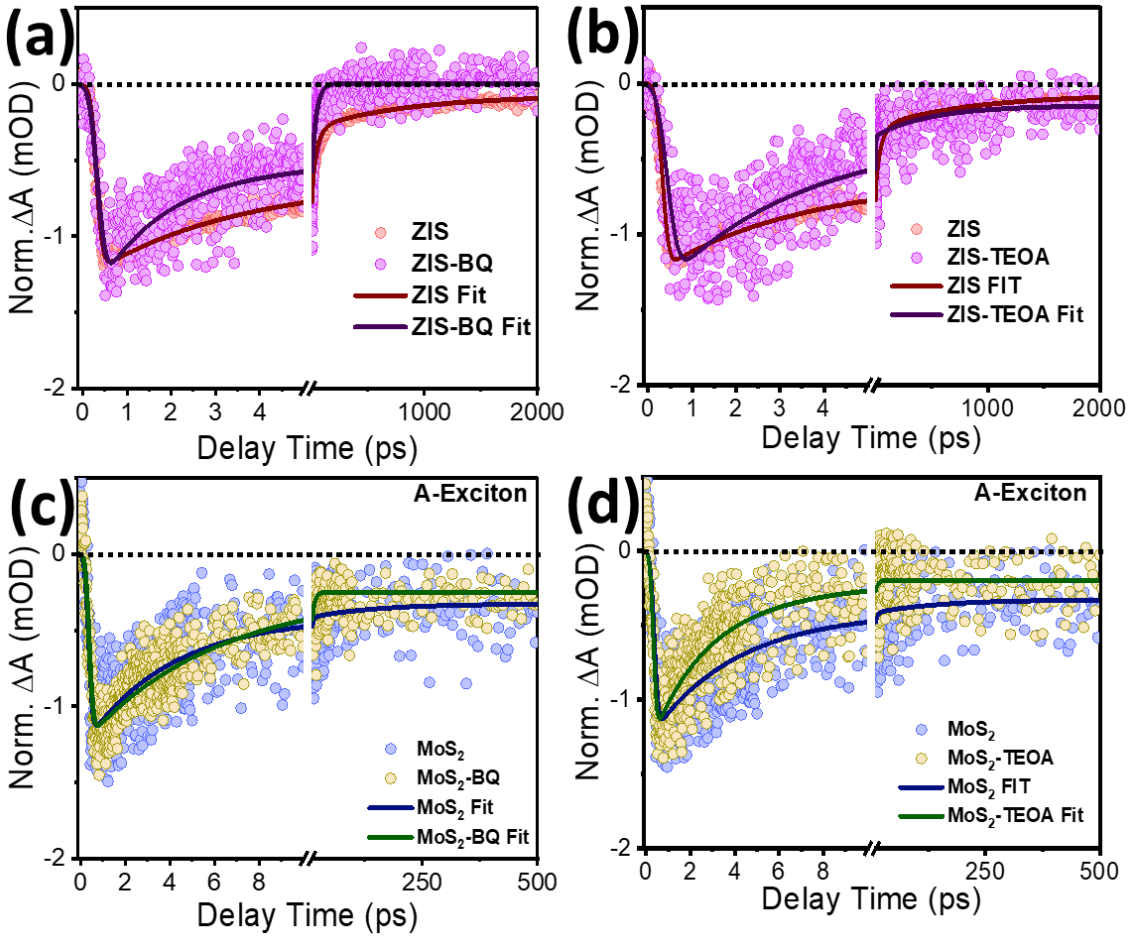

Figure S4. Comparative TA kinetics of pristine ZIS nanosheets with **(a)** electron quencher (benzoquinone) and **(b)** hole quencher (TEOA). Comparative TA kinetics of pristine MoS_2 with **(c)** electron quencher (benzoquinone) and **(d)** hole quencher (TEOA).

Table S4. Fitting parameters for TA kinetics of all the systems after the photoexcitation at 370 nm.

System	Wavelength(nm)	Time constant (τ)			
		τ_g (ps)	τ_1 (ps)	τ_2 (ps)	τ_3 (ns)
ZIS	420	0.2 (100%)	5.6 (-50%)	52.4 (-25%)	>1 (-25%)
ZIS/MoS_2-10	420	0.11 (100%)	2.7 (-66.7%)	30.2 (-20.8%)	>1 (-12.5%)
	687	0.25 (100%)	3.02 (-58.3%)	69.9 (-8.3%)	>1 (-33.4%)
MoS_2	687	0.15 (100%)	0.94 (-50%)	15.7 (-33.3%)	>1 (-16.7%)

References:

1 T. Goswami, D. K. Yadav, H. Bhatt, G. Kaur, A. Shukla, K. J. Babu and H. N. Ghosh, *J. Phys. Chem. Lett.*, 2021, **12**, 5000–5008.

2 Z. Zhang, L. Huang, J. Zhang, F. Wang, Y. Xie, X. Shang, Y. Gu, H. Zhao and X. Wang, *Appl. Catal. B*, 2018, **233**, 112–119.

3 K. Afroz, M. Moniruddin, N. Bakranov, S. Kudaibergenov and N. Nuraje, *J. Mater. Chem. A*, 2018, **6**, 21696–21718.

4 Q. Wang, T. Hisatomi, Q. Jia, H. Tokudome, M. Zhong, C. Wang, Z. Pan, T. Takata, M. Nakabayashi, N. Shibata, Y. Li, I. D. Sharp, A. Kudo, T. Yamada and K. Domen, *Nat. Mater.*, 2016, **15**, 611–615.

5 S. Zhang, X. Liu, C. Liu, S. Luo, L. Wang, T. Cai, Y. Zeng, J. Yuan, W. Dong, Y. Pei and Y. Liu, *ACS Nano*, 2018, **12**, 751–758.

6 Y. He, Z. Luo, T. Zhou, J. Zhang, Z. Zhu, Y. Zhang, G. Zhang and Q. Liu, *J. Colloid. Interface Sci.*, 2025, **684**, 481–491.

7 H. Yin, H. Chen, X. Feng, X. Chen, Q. Fei, Y. Zhang, Q. Zhao and Y. Zhang, *Int. J. Hydrogen Energy*, 2024, **51**, 433–442.

8 M. Zhao, S. Liu, D. Chen, S. Zhang, S. A. C. Carabineiro and K. Lv, *Chinese J. Catal.*, 2022, **43**, 2615–2624.

9 G. Zuo, Y. Wang, W. L. Teo, Q. Xian and Y. Zhao, *Appl. Catal. B*, 2021, **291**, 120126.

10 Y. Chen, L. Zhu, J. Li, L. Qiu, C. Zhou, X. Xu, Y. Shen, J. Xi, D. Men, P. Li and S. Duo, *Inorg. Chem.*, 2023, **62**, 7111–7122.

11 C. Cui, X. Xu, X. Zhao, N. Xi, M. Li, X. Wang, Y. Sang, X. Yu, H. Liu and J. Wang, *Nano Energy*, 2024, **126**, 109632.

12 S. Farhan, A. Hassan Raza, S. Yang, Z. Yu and Y. Wu, *J. Colloid. Interface Sci.*, 2024, **669**, 430–443.

13 X. Sun, M. Song, F. Liu, H. Peng, T. Zhao, S.-F. Yin and P. Chen, *Appl. Catal. B*, 2024, **342**, 123436.

14 Y. Chen, F. Su, H. Xie, R. Wang, C. Ding, J. Huang, Y. Xu and L. Ye, *Chem. Eng. J.*, 2021, **404**, 126498.

15 C.-H. Zhao, K.-L. Luo and W. Li, *Colloids Surf. A Physicochem. Eng. Asp.*, 2023, **671**, 131652.

16 X. Zhan, Y. Zheng, B. Li, Z. Fang, H. Yang, H. Zhang, L. Xu, G. Shao, H. Hou and W. Yang, *Chem. Eng. J.*, 2022, **431**, 134053.

17 C. Li, H. Che, P. Huo, Y. Yan, C. Liu and H. Dong, *J. Colloid. Interface Sci.*, 2021, **581**, 764–773.

18 K. Huang, C. Li and X. Meng, *J. Colloid. Interface Sci.*, 2020, **580**, 669–680.

19 B. Zhang, W. Xiao, J. Hu, J. Liu, H. Xu, X. Zheng, W. Wang, H. Wu, X. Xi, P. Dong and H. Ji, *J. Colloid. Interface Sci.*, 2023, **651**, 948–958.

20 P. Tan, M. Zhang, L. Yang, R. Ren, H. Zhai, H. Liu, J. Chen and J. Pan, *Diam. Relat. Mater.*, 2023, **140**, 110456.

21 O. Cavdar, M. Baluk, A. Malankowska, A. Żak, W. Lisowski, T. Klimczuk and A. Zaleska-Medynska, *J. Colloid. Interface Sci.*, 2023, **640**, 578–587.

22 S. Wang, X. Su, W. Han, G. Xu, D. Zhang, C. Su, X. Pu and P. Cai, *Int. J. Hydrogen Energy*, 2023, **48**, 21712–21722.

23 W. Gao, X. Zhao, T. Zhang, X. Yu, Y. Ma, E. C. dos Santos, J. White, H. Liu and Y. Sang, *Nano Energy*, 2023, **110**, 108381.

24 Y. Zhang, S. Guo, X. Xin, Y. Song, L. Yang, B. Wang, L. Tan and X. Li, *Appl. Surf. Sci.*, 2020, **504**, 144291.

25 J. Qiu, J. Pan, S. Wei, Q. Liang, Y. Wang, R. Wu and C. Li, *RSC Adv.*, 2021, **11**, 38523–38527.

26 J. E. Samaniego-Benitez, L. Lartundo-Rojas, A. García-García, H. A. Calderón and A. Mantilla, *Catal. Today*, 2021, **360**, 99–105.

27 T. Li, J.-D. Cui, L.-M. Gao, Y.-Z. Lin, R. Li, H. Xie, Y. Zhang and K. Li, *ACS Sustain. Chem. Eng.*, 2020, **8**, 13352–13361.